JPET Fast Forward. Published on September 17, 2021 as DOI: 10.1124/jpet.121.000786
This article has not been copyedited and formatted. The final version may differ from this version.

Selective acetyl-CoA carboxylase 1 inhibitor improves hepatic steatosis and hepatic fibrosis in a pre-clinical NASH model

Yumiko Okano Tamura, Jun Sugama, Shinji Iwasaki, Masako Sasaki, Hironobu Yasuno, Kazunobu Aoyama, Masanori Watanabe, Derek M. Erion, Hiroaki Yashiro

Cardiovascular and Metabolic Drug Discovery Unit, Takeda Pharmaceutical Company Limited, Kanagawa, Japan (YOT, JS, MW)

Drug Metabolism & Pharmacokinetics Research Laboratories, Takeda Pharmaceutical Company Limited, Kanagawa, Japan (SI, KA)

Biomolecular Research Laboratories, Takeda Pharmaceutical Company Limited, Kanagawa, Japan (MS)

Drug Safety Research Laboratories, Takeda Pharmaceutical Company Limited, Kanagawa, Japan (HY)

Gastroenterology Drug Discovery Unit, Takeda Pharmaceutical Company Limited, Cambridge, USA (DME, HY)

JPET Fast Forward. Published on September 17, 2021 as DOI: 10.1124/jpet.121.000786
This article has not been copyedited and formatted. The final version may differ from this version.

Running title: ACC1 inhibitor improves hepatic steatosis and fibrosis

*** Corresponding author:**

Name: Hiroaki Yashiro

Address: Gastroenterology Drug Discovery Unit

Takeda Pharmaceuticals International Co.

350 Massachusetts Avenue,

Cambridge, MA 02139, USA

Tel.: 617.444.4360

E-mail address: hiroaki.yashiro@takeda.com

Number of text pages: 23

Number of tables: 2

Number of figures: 6

Number of references: 40

Number of words in the Abstract: 212

Number of words in the Introduction: 744

Number of words in the Discussion: 1301

List of abbreviations:

JPET Fast Forward. Published on September 17, 2021 as DOI: 10.1124/jpet.121.000786
This article has not been copyedited and formatted. The final version may differ from this version.

ACC	Acetyl-CoA carboxylase
ALT	Alanine aminotransferase
AST	Aspartate aminotransferase
BW	Body weight
DMEM	Dulbecco's modified Eagle medium
DNL	*De novo* lipogenesis
FAS	Fatty acid synthase
FI	Food intake
HTR2B	5-hydroxytryptamine receptor 2B
KO	Knockout
M-CoA	Malonyl-CoA
MC	Methylcellulose
MC4R	Melanocortin 4 receptor
NAFLD	Nonalcoholic fatty liver disease
NASH	Nonalcoholic steatohepatitis
PG	Plasma glucose
TC	Total cholesterol
TG	Triglyceride
WD	Western diet

JPET Fast Forward. Published on September 17, 2021 as DOI: 10.1124/jpet.121.000786
This article has not been copyedited and formatted. The final version may differ from this version.

WT	Wild-type

Section assignment: Gastrointestinal, Hepatic, Pulmonary, and Renal

JPET Fast Forward. Published on September 17, 2021 as DOI: 10.1124/jpet.121.000786
This article has not been copyedited and formatted. The final version may differ from this version.

Abstract

Acetyl-CoA carboxylase (ACC) 1 and ACC2 are essential rate-limiting enzymes that synthesize malonyl-CoA (M-CoA) from acetyl-CoA. ACC1 is predominantly expressed in lipogenic tissues and regulates the *de novo* lipogenesis flux. It is upregulated in the liver of patients with nonalcoholic fatty liver disease (NAFLD), ultimately leading to the formation of fatty liver. Therefore, selective ACC1 inhibitors may prevent the pathophysiology of NAFLD and nonalcoholic steatohepatitis (NASH) by reducing hepatic fat, inflammation, and fibrosis. Many studies have suggested ACC1/2 dual inhibitors for treating NAFLD/NASH; however, reports on selective ACC1 inhibitors are lacking. In this study, we investigated the effects of compound-1, a selective ACC1 inhibitor for treating NAFLD/NASH, using pre-clinical *in vitro* and *in vivo* models. Compound-1 reduced M-CoA content and inhibited the incorporation of [^{14}C] acetate into fatty acids in HepG2 cells. Additionally, it reduced hepatic M-CoA content and inhibited DNL in C57BL/6J mice after a single dose. Further, compound-1 treatment for 8 weeks in western diet-fed melanocortin 4 receptor knockout mice—NAFLD/NASH mouse model—improved liver hypertrophy and reduced hepatic triglyceride content. The reduction of hepatic M-CoA by the selective ACC1 inhibitor was highly correlated with the reduction in hepatic steatosis and fibrosis. These findings support further investigations of the use of this ACC1 inhibitor as a new treatment for NFLD/NASH.

Significance statement:

This is the first study to demonstrate that a novel selective inhibitor of acetyl-CoA carboxylase 1 (ACC1)

JPET Fast Forward. Published on September 17, 2021 as DOI: 10.1124/jpet.121.000786
This article has not been copyedited and formatted. The final version may differ from this version.

has anti-nonalcoholic fatty liver disease (NAFLD) and anti-nonalcoholic steatohepatitis (NASH) effects in pre-clinical models. Treatment with this compound significantly improved hepatic steatosis and fibrosis in a mouse model. These findings support the use of this ACC1 inhibitor as a new treatment for NAFLD/NASH.

JPET Fast Forward. Published on September 17, 2021 as DOI: 10.1124/jpet.121.000786
This article has not been copyedited and formatted. The final version may differ from this version.

Introduction

Nonalcoholic fatty liver disease (NAFLD) is a liver disease characterized by excessive fat accumulation in hepatocytes that is not caused by alcohol consumption (Friedman et al., 2018; Vernon et al., 2011). Nonalcoholic steatohepatitis (NASH) is a sub-category of NAFLD and is defined on the basis of the following liver biopsy histological features: lobular inflammation, hepatocellular ballooning, fibrosis, and steatosis (Williams et al., 2011; Siddiqui et al., 2018). Since NAFLD and NASH are associated with cirrhosis and hepatocellular carcinoma (Anstee, 2013), they also represent important factors that contribute to the recent increase in liver-related morbidity and mortality.

The global prevalence of NAFLD has continued to increase annually with 25% of the world population affected in 2018 (Younossi et al., 2019). Although up to 30% of the patients with NAFLD develop NASH (Calzadilla Bertot and Adams, 2016), no anti-NAFLD/NASH drugs have been approved (Sanyal et al., 2010; Cusi et al., 2016; Esler and Bence, 2019), thus resulting in an unmet medical need. Hepatic steatosis is caused by an imbalance in hepatic lipid metabolism favoring the storage of lipids within the liver (Cohen et al., 2011), which triggers hepatic inflammation and, subsequently, fibrosis, which drives NASH progression. Furthermore, metabolic syndromes, such as obesity, insulin resistance, and dyslipidemia, represent the major risk factors for the development of NAFLD/NASH. Therefore, multiple clinical trials are focusing on correcting the dysfunctional lipid metabolism via the application of lipid metabolism pathway modulators, nuclear hormone receptor agonists, and glycemic modulators (Esler and Bence, 2019).

JPET Fast Forward. Published on September 17, 2021 as DOI: 10.1124/jpet.121.000786
This article has not been copyedited and formatted. The final version may differ from this version.

Acetyl-CoA carboxylase (ACC) is an essential rate-limiting enzyme in fatty acid metabolism that catalyzes the carboxylation of acetyl-CoA to form malonyl-CoA (M-CoA) (Brownsey et al., 1997). Mammals have two ACC isoforms. ACC1 is localized in the cytosol and predominantly expressed in lipogenic tissues, such as the liver and adipose tissue; whereas ACC2 is localized in the mitochondrial surface and is predominantly expressed in oxidative tissues, including skeletal muscle and heart, and to some extent, in the liver and adipose tissues (Abu-Elheiga et al., 2001). M-CoA produced by ACC1 is an intermediate in *de novo* lipogenesis (DNL) and acts as a substrate for fatty acid synthase (FAS) in acyl chain elongation (Mao et al., 2006). Furthermore, M-CoA produced by ACC2 inhibits carnitine palmitoyltransferase 1, which participates in regulating fatty acid β-oxidation (Abu-Elheiga et al., 2001, 2003). Indeed, several studies have shown that liver-specific ACC1 knockout (KO) mice have reduced hepatic DNL, M-CoA, and triglyceride (TG) accumulation (Mao et al., 2006; Harada et al., 2007), whereas ACC2 KO mice exhibit increased fatty acid oxidation coupled with elevated whole-body energy expenditure and improved whole-body adiposity compared to wild-type mice (Choi et al., 2007; Abu-Elheiga et al., 2001).

Recently, several ACC1/2 dual inhibitors have been investigated for treating NAFLD/NASH in pre-clinical and clinical studies (Chen et al., 2019; Esler et al., 2019), many of which have reported that these dual inhibitors induce undesirable effects, including plasma TG elevation, which may be caused by excessive suppression of ACC activity. However, the anti-NAFLD/NASH effect of selective ACC1 inhibitors has not been evaluated in pre-clinical or clinical studies to understand whether the therapeutic

JPET Fast Forward. Published on September 17, 2021 as DOI: 10.1124/jpet.121.000786
This article has not been copyedited and formatted. The final version may differ from this version.

window for ACC1 inhibitors would be greater than that for ACC1/2 inhibitors.

To support the efficacy of an ACC1 inhibitor, selective ACC1 suppression using antisense oligonucleotides demonstrated both reduced triglyceride synthesis and increased fat oxidation in primary rat hepatocytes (Savage et al., 2006). Furthermore, hepatic DNL is markedly higher in patients with NAFLD than in healthy subjects (Donnelly et al., 2005; Fabbrini et al., 2008; Lambert et al., 2014). Lastly, ACC1, not ACC2, expression has been reported as upregulated in the liver of NAFLD patients (Kohjima et al., 2007). These data suggest that ACC1 inhibition alone could have the potential to improve hepatic steatosis and fibrosis.

Recently, Mizojiri et al. (2018) generated a systemic selective human ACC1 inhibitor, compound-1 (selectivity more than 17,000-fold over that for human ACC2). To investigate the anti-NAFLD/NASH effect of ACC1 inhibition, we evaluated the effect of compound-1 on M-CoA production and hepatic DNL *in vitro* and *in vivo*. Additionally, we investigated the effects of compound-1 on hepatic steatosis and fibrosis by using western diet (WD)-fed melanocortin 4 receptor (MC4R) KO mice, a genetic and obesogenic dietary model that mimics the human pathophysiology of NAFLD/NASH with obesity, insulin resistance, and excessive lipid accumulation, as well as enhanced liver fibrosis (Itoh et al., 2011; Konuma et al., 2015; Shiba et al., 2018). Taken together, these data are supportive of the critical role of ACC1 in the pathophysiology of liver diseases.

JPET Fast Forward. Published on September 17, 2021 as DOI: 10.1124/jpet.121.000786
This article has not been copyedited and formatted. The final version may differ from this version.

Materials and Methods

Compounds

Compounds used in the study were synthesized by Takeda Pharmaceutical Company Limited (Kanagawa, Japan). In the animal studies, compounds were suspended in 0.5% methylcellulose (MC).

Mouse and human ACC enzyme assays

Compounds were dissolved in dimethyl sulfoxide (DMSO) and then diluted with an enzyme reaction buffer [50 mM HEPES (pH 7.5), 10 mM $MgCl_2$, 10 mM tripotassium citrate, 2 mM dithiothreitol, and 0.001% fatty acid-free bovine serum albumin]. Recombinant mouse ACC1 or ACC2 produced by Sf-9 cells was diluted with the enzyme reaction buffer to 0.8 μg/mL and 0.1 μg/mL, respectively. A 5 μL-aliquot of the compound solution was added to each well of a 384-well assay plate, and 10 μL of the enzyme mixture was added to each well. The mixture was incubated at room temperature for 60 min. Next, a substrate solution (50 mM $KHCO_3$, 200 μM ATP, and 5 μL of 200 μM acetyl-CoA) was added to each well, and the mixture was reacted at room temperature for 15 min. The reaction was stopped by adding 40 μL of stop solution (1.3% formic acid, 0.2 μM malonyl-$^{13}C_3$-CoA; 655759; Fujifilm Wako Pure Chemical Industries, Osaka, Japan) to each of the obtained reaction mixtures. The production of M-CoA was detected using RapidFire mass spectrometry (API4000; Sciex, Tokyo, Japan) and corrected with malonyl-$^{13}C_3$-CoA. The IC_{50} values were calculated using XLfit from the data expressed as inhibition (%) by using fit Model 204 (4 Parameter Logistic Model). The IC_{50} values of the inhibitors were converted to

JPET Fast Forward. Published on September 17, 2021 as DOI: 10.1124/jpet.121.000786
This article has not been copyedited and formatted. The final version may differ from this version.

pIC_{50} [log ($1/IC_{50}$)] and used as the dependent variable for correlation analysis. The response of vehicle control was considered as 0% inhibition, and that without enzyme was considered as 100% inhibition. The human ACC enzyme assay was performed following the protocol reported in a previous study (Mizojiri et al., 2018).

Cell culture

The human hepatoma-derived cell line, HepG2, was purchased from the American Type Culture Collection (HB-8065; Manassas, VA, USA). The cells were incubated in Dulbecco's modified Eagle medium (DMEM) (10567014; Thermo Fisher Scientific, Tokyo, Japan) containing 10% fetal bovine serum (SH30084.03; Hyclone Laboratories Inc., Logan, UT, USA), penicillin, and streptomycin under 5% CO_2 at 37 ℃.

Measurement of M-CoA content in HepG2 cells

HepG2 cells were plated in a 12-well plate at 2.4×10^5 cells/well and incubated for 48 h under 5% CO_2 at 37 ℃. After the medium was removed, cells were incubated with DMSO or compound-1 in the assay medium (DMEM containing 0.09% fatty acid-free bovine serum; 017-22231; Fujifilm Wako Pure Chemical Industries, Osaka, Japan) for 2 h. Next, the cells were washed with 500 μL of ice-cold phosphate-buffered saline (PBS), and 1200 μL of ice-cold 6% hydrogen peroxide was added to lyse the cells. After the cell lysates were collected in tubes, samples were immediately stored at -80 ℃ until

JPET Fast Forward. Published on September 17, 2021 as DOI: 10.1124/jpet.121.000786
This article has not been copyedited and formatted. The final version may differ from this version.

analysis. Refer to the experimental section on M-CoA for the measurements.

Measurement of DNL in HepG2 cells

HepG2 cells were plated in a 24-well plate at 1.5×10^5 cells/well and incubated for 24 h under 5% CO_2 at 37 ℃. The cells were washed twice with 500 μL of PBS and incubated with DMSO or compound-1 in assay medium (DMEM containing 0.09% fatty acid-free bovine serum) for 1 h. Subsequently, 5 μL of ^{14}C-acetate (25 mM, 10 μCi/μmol) was added and incubated for 2 h at 37 ℃. After the cells were washed twice with 500 μL of PBS, 500 μL of 0.5 N NaOH was added to lyse the cells. Next, 200 μL of 50% KOH and 1000 μL of EtOH were added to the cell lysate and incubated for 1 h at 70 ℃ for saponification. Next, 1000 μL of H_2O was added, followed by the addition of 4000 μL of petroleum ether. After the organic layers were collected, HCl was added to the aqueous layer to adjust the pH to below 4. Subsequently, 4000 μL of petroleum ether was added, and the organic layers were collected. The pooled organic layers were dried using N_2 gas and resuspended in a scintillation A cocktail. Radioactivity was measured using liquid scintillation counting in 3110 TR (PerkinElmer Inc., Waltham, MA, USA).

Animals

Animal experiments were approved by the Institutional Animal Care and Use Committee of Shonan Research Center, Takeda Pharmaceutical Company Limited (Kanagawa, Japan), and conformed to the guidelines of the US National Institutes of Health—Guide for the Care and Use of Laboratory Animals.

JPET Fast Forward. Published on September 17, 2021 as DOI: 10.1124/jpet.121.000786
This article has not been copyedited and formatted. The final version may differ from this version.

Male C57BL/6J mice were purchased from Charles River Laboratories, Japan (Yokohama, Japan) and fed normal chow (CE-2; CLEA Japan, Inc., Tokyo, Japan). Male Mc4r null (MC4R KO) mice were generated following a previous study (Matsumoto et al., 2020). MC4R KO mice and wild-type littermate mice were fed CE-2. All animals were housed in a group under controlled conditions including a 12 h/12 h light/dark cycle at 20–26 ℃ and humidity of 40–70%; they were allowed free access to food and tap water.

Evaluation of the effect of a single dose of compound-1 on hepatic M-CoA in CE-2-fed C57BL/6J mice (dose-response study)

For this, 7-week-old CE-2-fed C57BL/6J mice were divided into eight groups of five mice each based on body weight (BW) and BW change during habituation. Mice were orally administered (10 mL/kg volume) with vehicle (0.5% MC), compound-1, or compound-2, and sacrificed after 2 h of treatment under isoflurane anesthesia. Blood samples were collected from the abdominal vena cava and centrifuged at 13,000 × *g* for 5 min at 4 ℃ to collect plasma, which was stored at −80 ℃ for pharmacokinetic analysis. After the liver weight was measured, liver samples were immediately frozen in liquid nitrogen and stored at −80 ℃ for M-CoA measurement and pharmacokinetic (PK) analysis. Refer to the M-CoA and PK experimental section for the measurements.

Evaluation of the effect of a single dose of compound-1 on hepatic DNL in WD-fed C57BL/6J mice

JPET Fast Forward. Published on September 17, 2021 as DOI: 10.1124/jpet.121.000786
This article has not been copyedited and formatted. The final version may differ from this version.

For this, 7-week-old mice were divided into four groups of three mice each based on BW after they were fed WD (D12079B; Research Diets, Inc., New Brunswick, NJ, USA) for 3 days. Mice were orally administered (10 mL/kg volume) vehicle (0.5% MC) or compound-1 (10 mg/kg) and intraperitoneally administered ^{14}C-acetate (400 μCi/5 mL/kg) after 1 h of treatment. Mice were sacrificed after 2 or 5 h of drug treatment under isoflurane anesthesia. The radioactivity of the fatty acid fraction in the liver was measured according to a previous study (Harwood et al., 2003).

Repeated dose study of compound-1 in WD-fed MC4R KO mice

For this, 9-week-old MC4R KO mice were fed WD, and wild-type (WT) mice were fed CE-2. At the age of 23 weeks, WD-fed MC4R KO mice were divided into four groups of eight mice each based on BW, food intake (FI), plasma glucose (PG), triglyceride (TG), total cholesterol (TC), aspartate aminotransferase (AST), alanine aminotransferase (ALT), and insulin at day −3. Mice were orally administered (5 mL/kg volume) vehicle (0.5% MC) or compound-1 (3, 10, and 30 mg/kg) once daily for 8 weeks.

BW and FI were monitored every 3–4 days. On days 17, 31, and 56, blood samples were collected from the tail vein for the measurement of plasma parameters. PG, TG, TC, AST, and ALT were enzymatically measured using an Autoanalyzer 7180 (Hitachi High-Technologies Corporation, Tokyo, Japan). Plasma insulin levels were measured using sandwich enzyme-linked immunosorbent assay (ELISA; Shibayagi, Gunma, Japan, or Morinaga Institute of Biological Science, Kanagawa, Japan).

For pharmacokinetic analysis, blood samples were collected from the tail vein at day 56. Blood

JPET Fast Forward. Published on September 17, 2021 as DOI: 10.1124/jpet.121.000786
This article has not been copyedited and formatted. The final version may differ from this version.

samples were centrifuged at 13,000 × *g* for 5 min at 4 ℃ to collect plasma, which was stored at −80 ℃ for pharmacokinetic analysis. Refer to the PK experimental section for the measurements.

Mice were sacrificed under isoflurane anesthesia on day 0 (pre) and day 60. Blood samples were collected from the abdominal vena cava and centrifuged at 13,000 × *g* for 5 min at 4 ℃ to collect plasma, which was stored at −80 ℃ for the measurement of parameters. After the liver weight was measured, liver samples were immediately frozen in liquid nitrogen and stored at −80 ℃. For histopathological analysis, liver samples were stored in 10% neutral buffered formalin.

The hepatic TG content was measured as follows. First, 900 μL of saline was added to 100 mg liver tissue and homogenized (27 Hz, 2 min) with zirconia beads. The homogenate (200 μL) was mixed thoroughly with 600 μL of $CHCl_3$:MeOH (1:2) for 30 min. After 200 μL of $CHCl_3$ and 200 μL of H_2O were added to the mixed homogenate, it was stirred for 10–30 min. After centrifugation (12,000 × *g*, 2 min, room temperature), the $CHCl_3$ layers were collected, and 50 μL was dried under N_2 gas and resuspended in isopropanol (80 μL for WT mice sample and 300 μL for MC4R KO mice sample). Extracted triglyceride content was measured using the Triglyceride-E test (432-40201; Fujifilm Wako Pure Chemical Industries, Osaka, Japan).

The hepatic collagen levels were measured using a commercially available kit (QZBTOTCOL1; Quickzyme Biosciences, Leiden, Netherlands) according to manufacturer's instructions.

The percentage of hepatic Sirius red-positive area was measured as follows. Liver samples fixed with 10% neutral buffered formalin were embedded in paraffin. Liver histology was assessed in 4-μm-thick

JPET Fast Forward. Published on September 17, 2021 as DOI: 10.1124/jpet.121.000786
This article has not been copyedited and formatted. The final version may differ from this version.

sections stained with hematoxylin-eosin (HE) and Sirius red. The Sirius red-positive areas were quantified using four randomly selected fields per liver sample by using the WinROOF software (Mitani Co., Tokyo, Japan). Histological analysis was conducted in a randomized and double-blinded manner.

Hepatic mRNA levels were measured as follows. Total RNA was isolated from the liver samples that were stored in RNA later by using a Lipid Tissue Mini kit (Qiagen, Tokyo, Japan). Reverse transcription reactions were performed using a SuperScript VILO cDNA synthesis kit (Thermo Fisher Scientific, Tokyo, Japan), according to manufacturer's instructions. Gene expression was quantified using TaqMan real-time PCR (ABI7900; Thermo Fisher Scientific, Tokyo, Japan) using Platinum qPCR SuperMix-UDG (Thermo Fisher Scientific, Tokyo, Japan) and primers/Taqman probe sets (Thermo Fisher Scientific, Tokyo, Japan). The following primer-probe sets were used: monocyte chemoattractant protein-1 (*Ccl2*; *MCP-1*, Mm00441242_m1), *Adgre1* (*F4/80*, Mm00802529_m1), collagen type1 alpha1 (*Col1α1*; Mm00801666_g1), collagen type1 alpha2 (*Col1α2*; Mm00483888_m1), alpha-smooth muscle actin (*Acta2; αSMA,* Mm00725412_s1), transforming growth factor-beta 1 (*Tgfβ1*; *TGF-β1*, Mm01178820_m1), acetyl-coenzyme A carboxylase alpha (*Acaca*; *ACC1*, Mm01304257_m1), acetyl-coenzyme A carboxylase beta (*Acacb*; *ACC2*, Mm01204671_m1), FAS (*Fasn*; Mm00662319_m1), stearoyl-coenzyme A desaturase 1 (*Scd1*; Mm00772290_m1), and *Rplp0* (*36B4*, Mm00725448_s1). The relative gene expression was calculated using the ΔΔCt method and normalized to *Rplp0* expression.

Measurement of cellular or hepatic M-CoA

JPET Fast Forward. Published on September 17, 2021 as DOI: 10.1124/jpet.121.000786
This article has not been copyedited and formatted. The final version may differ from this version.

Tissue samples were homogenized in 6% perchloric acid containing malonyl-$^{13}C_3$-CoA (Sigma-Aldrich, St. Louis, MO, USA) as an internal standard. After centrifugation, the supernatant was subjected to solid-phase extraction by using an Oasis HLB Extraction Cartridge (Waters, Milford, MA, USA). The analyte was eluted with acetonitrile and supplemented with dibutylammonium acetate (Tokyo Chemical Industries, Tokyo, Japan), followed by rinsing of the column with ultrapure water. The eluate was dried under a stream of nitrogen, and the residue was reconstituted in 100 μL of ultrapure water. An aliquot of 10 μL was injected into the liquid chromatography-tandem mass spectrometry (LC-MS/MS) system, which consisted of a Shimadzu LC-20AD HPLC system (Shimadzu, Kyoto, Japan) and an API5000 or API5500 mass spectrometer (AB Sciex, Foster City, CA, USA). The analytical column was a CAPCELL CORE C18 column (2.7 μm, 2.1 × 50 mm; Shiseido, Kanagawa, Japan) used at 40 ℃. The mobile phases consisted of (A) 50 mM ammonium carbonate/ammonium hydroxide (pH 9) supplemented with dibutylammonium acetate and (B) acetonitrile. The analyte was eluted using a gradient of 95% solvent A/5% solvent B to 5% solvent A/95% solvent B. The flow rate of the mobile phase was 0.3 mL/min. Detection was performed using multiple reaction monitoring in the positive ionization mode [selected reaction monitoring m/z = 854.1 → 347.1 or 854.1 → 303.3 for M-CoA and m/z = 857.2 → 350.2 for malonyl-$^{13}C_3$-CoA (internal standard)]. Analyst™ software (version 1.6.2, AB Sciex) was used for data acquisition and processing. The concentration of compounds in each sample was back-calculated using a calibration curve generated from a series of calibration standards.

JPET Fast Forward. Published on September 17, 2021 as DOI: 10.1124/jpet.121.000786
This article has not been copyedited and formatted. The final version may differ from this version.

Statistical analysis

All data in the graph are represented as means ± SDs. Statistical analyses were performed in EXSUS ver.8.0 in combination with SAS ver. 9.3 or GraphPad PRISM software. To evaluate the effects of compound-1 *in vivo*, we analyzed the statistical differences between vehicle and drug treatment in C57BL/6J mice or MC4R KO mice using Student's *t*-test, Aspin–Welch test, Dunnett's test, and Steel's test. To confirm the establishment of the disease state, we analyzed the statistical differences between WT mice and vehicle by using Student's *t*-test or Aspin–Welch test. For all tests, p-values of <0.05 were considered statistically significant. The correlation between hepatic M-CoA content and hepatic TG, hepatic M-CoA content and hepatic collagen were analyzed using Pearson's correlation coefficient.

JPET Fast Forward. Published on September 17, 2021 as DOI: 10.1124/jpet.121.000786
This article has not been copyedited and formatted. The final version may differ from this version.

Results

Inhibition of mouse ACC1 and ACC2

The inhibitory activities of compound-1 and compound-2 (dual ACC1/2 inhibitor) (Kamata et al., 2012) on recombinant mouse ACC1 and ACC2 enzymes were evaluated. Compound-1 inhibited recombinant human ACC1 and ACC2 at IC_{50} values of 0.58 nM and > 10,000 nM, respectively (Mizojiri et al., 2018), as well as mouse ACC1 and ACC2 with IC_{50} values of 1.9 nM and > 10,000 nM, respectively (Table 1). Conversely, compound-2 inhibited mouse ACC1 and ACC2 with IC_{50} values of 6.0 nM and 6.4 nM, respectively. These results indicate that compound-1 is selective for ACC1 inhibition, whereas compound-2 inhibits both ACC1 and ACC2.

Effect of compound-1 on M-CoA content and DNL in HepG2 cells

To assess the effect of compound-1 on M-CoA content and DNL in cultured cells, we investigated the effect of compound-1 on M-CoA production and [^{14}C] acetate incorporation into fatty acids in HepG2 cells. Compound-1 decreased the M-CoA content in cells with IC_{50} of 16.0 nM (Figure 1A) and inhibited [^{14}C] acetate incorporation into fatty acids with IC_{50} of 12.7 nM (Figure 1B) in a dose-dependent manner. In addition, the unbound fraction of compound-1 in the medium was 0.09. The estimated unbound compound-1-based IC_{50} when compound-1 inhibited M-CoA production and [^{14}C] acetate incorporation was 1.44 nM and 1.14 nM, respectively.

JPET Fast Forward. Published on September 17, 2021 as DOI: 10.1124/jpet.121.000786
This article has not been copyedited and formatted. The final version may differ from this version.

Effect of compound-1 on hepatic M-CoA content and DNL in C57BL/6J mice

M-CoA is formed from acetyl-CoA by ACC, and the hepatic M-CoA level could be used as a pharmacodynamic marker of ACC inhibition (Harriman et al., 2016; Glien et al., 2011). Therefore, we assessed the ability of compound-1 to suppress hepatic M-CoA content in C57BL/6J mice, which were fed normal chow. At 2 h after a single dose, compound-1 significantly and dose-dependently decreased hepatic M-CoA content from the lowest tested dose of 0.3 mg/kg. The efficacy of compound-1 tended to plateau at approximately 30 mg/kg, and a maximum reduction of −64% was noted at 100 mg/kg (Figure 2A). Conversely, compound-2 (100 mg/kg, to achieve >85% inhibition), an ACC1/2 dual inhibitor, reduced hepatic M-CoA by 88% compared to vehicle (Figure 2A). To analyze the correlation between compound-1 blood exposure and hepatic M-CoA reduction, we measured the plasma concentration of compound-1 at 2 h after dose. We already confirmed that the plasma and hepatic concentrations of compound-1 were similar in a separate time-course study. Thus, the plasma concentration can be used as the index for analyzing the pharmacokinetics and pharmacodynamics (data not shown). The IC_{50} of hepatic M-CoA reduction was 1.88 μg/mL (0.90 mg/kg) of plasma concentration in C57BL/6J mice (Supplementary Table 1). The exploratory *in vitro* study suggested high plasma protein binding of compound-1 to mice plasma and the estimated unbound compound-1-based IC_{50} was less than 5 nM. We also confirmed that compound-1 (10 mg/kg) did not change the M-CoA content in muscles where ACC2 is predominantly expressed 1 h after a single dose (data not shown).

To assess DNL inhibition by compound-1 *in vivo*, we evaluated the inhibition of [^{14}C] acetate

incorporation into fatty acids in mice that were fed WD. Compound-1 (10 mg/kg) inhibited hepatic fatty acid synthesis in WD-fed C57BL/6J mice by 77.6% and 67.8% at 2 and 5 h after oral administration, respectively (Figure 2B).

Based on these pharmacodynamic results, we selected the doses of 3, 10, and 30 mg/kg for the repeated dose study to investigate the anti-NAFLD/NASH effect of compound-1 in WD-fed MC4R KO mice.

Compound-1 improves hepatic steatosis and fibrosis in WD-fed MC4R KO mice

To evaluate the effects of compound-1 on NAFLD/NASH, we orally administered compound-1 to WD-fed MC4R KO mice once daily for 8 weeks at doses of 3, 10, and 30 mg/kg.

The liver weight and hepatic TG content in WD-fed MC4R KO mice were significantly higher than those in WT mice (Figure 3A and 3B). The total liver weights in compound-1 (3, 10, and 30 mg/kg)-treated groups were reduced by 9.1%, 23.8%, and 57.1%, respectively, compared to that in the vehicle-treated group (Figure 3A). In addition, consistent with the improvement of the appearance of fatty liver (data not shown), compound-1 significantly reduced the total hepatic TG at doses of 10 and 30 mg/kg (Figure 3B). These results indicate that compound-1 improves liver hypertrophy and steatosis.

All animals in the compound-1 (30 mg/kg)-treated group showed abnormal findings, such as dryness of the tail, loss of fur around the chest, and flushing of the face on day 56 (data not shown). No other abnormalities were observed in terms of anatomy and appearance. Only at 30 mg/kg did compound-1

JPET Fast Forward. Published on September 17, 2021 as DOI: 10.1124/jpet.121.000786
This article has not been copyedited and formatted. The final version may differ from this version.

treatment significantly decrease BW without reducing the cumulative FI (Figure 3C and 3D); however, the BW reduction was not correlated with the severity of skin toxicity.

The plasma parameter levels were evaluated before and after the 8-week treatment of compound-1 (Table 2). At the start of drug treatment, plasma AST and ALT, which are hepatic enzymes that could be used as markers of hepatocellular injury (Zechini et al., 2004), and TC levels were higher in WD-fed MC4R KO mice than in WT mice. In contrast, plasma TG levels were lower in WD-fed MC4R KO mice than in WT mice. These data suggested that WD-fed MC4R KO mice exhibited hepatocellular injury and lipid metabolism disruption.

Compound-1 treatment markedly decreased plasma AST, ALT, and TC levels in a dose-dependent manner, whereas the treatment increased plasma TG concentrations compared to those in the vehicle-treated group. However, plasma TG levels in the compound-1-treated mice never reached statistically significant increased values over those observed in the WT mice.

The plasma concentration and pharmacokinetic parameters of compound-1 before and after the final dose are shown in Supplementary Table 2.

To evaluate the effects of compound-1 on markers of inflammation and fibrosis, we measured the mRNA expression of *MCP-1* and *F4/80* as markers of inflammation and that of *Col1α1*, *Col1α2*, *αSMA*, and *TGF-β1* as markers of fibrosis activity in the liver. In addition, we evaluated the expression of lipogenesis-related genes, including *ACC1* and *ACC2* in the liver. Compared to WT mice, WD-fed, vehicle-treated MC4R KO mice showed remarkable elevation in the expression levels of *MCP-1*, *F4/80*,

JPET Fast Forward. Published on September 17, 2021 as DOI: 10.1124/jpet.121.000786
This article has not been copyedited and formatted. The final version may differ from this version.

Col1α1, *Col1α2*, *αSMA*, and *TGF-β1* (Figure 4), suggesting progression to NASH with macrophage infiltration induced by MCP-1 which are hypothesized to be induced by hepatic steatosis, were observed in this mouse model. In addition, we confirmed that the expression of *ACC1*, *Fasn*, and *Scd1* was increased in this model (Supplementary Figure 1); these are consistent with the findings of previous studies (Itoh et al., 2011; Konuma et al., 2015; Shiba et al., 2018). Compound-1 significantly decreased the gene expression levels of *MCP-1*, *F4/80*, *Col1α1*, *Col1α2*, *αSMA*, and *TGF-β1* (Figure 4), whereas it increased those of *ACC1*, *ACC2*, *Fasn*, and *Scd1* (Supplementary Figure 1).

We measured the hepatic M-CoA content as a PD marker at 20 h after the final dose in WD-fed MC4R KO mice. Compound-1 dose-dependently reduced hepatic M-CoA content, and the maximum efficacy was observed in the 30 mg/kg group, which was 62% lower than that in the vehicle-treated group (Figure 5).

In addition, we investigated the anti-fibrotic effect of compound-1 by conducting biochemical and histological analyses in the liver. Hepatic collagen content and Sirius red-positive area were significantly higher in WD-fed MC4R KO mice than in WT mice (Figure 6A, 6B, and 6C). Compound-1 significantly decreased hepatic collagen (mg/liver) at doses of 10 and 30 mg/kg and Sirius red-positive area at doses of 3 and 10 mg/kg. Notably, hepatic M-CoA reduction was correlated with the decrease in hepatic TG and collagen (Figure 6D and 6E, $R^2 = 0.5716$ ****$p < 0.0001$ and $R^2 = 0.5472$ ****$p < 0.0001$).

JPET Fast Forward. Published on September 17, 2021 as DOI: 10.1124/jpet.121.000786
This article has not been copyedited and formatted. The final version may differ from this version.

Discussion

Hepatic DNL is markedly higher in NAFLD patients than in healthy individuals (Donnelly et al., 2005; Fabbrini et al., 2008; Lambert et al., 2014), and ACC1—the rate-limiting enzyme for hepatic DNL—is upregulated in NAFLD patients (Kohjima et al., 2007), suggesting that abnormal ACC1 activity contributes to the pathogenesis of fatty liver, a key feature of NAFLD. In the current study, compound-1, a novel selective ACC1 inhibitor, was found to influence hepatic M-CoA concentrations, which in turn reduced hepatic lipid accumulation and prevented hepatic fibrosis in WD-fed MC4R KO mice.

First, we determined that compound-1 is highly selective, at the enzyme level, for mouse ACC1, not ACC2, thus providing a candidate molecule for further studies on the biological function of ACC1. We also confirmed the effect of compound-1 on the pharmacodynamic marker M-CoA in a liver cell model indicating that ACC1 inhibition is sufficient to reduce intracellular M-CoA concentrations. The cellular M-CoA production and subsequent fatty acid synthesis were dose-dependently suppressed by compound-1 treatment. Therefore, compound-1 inhibits M-CoA content and fatty acid synthesis in hepatocytes by selectively blocking ACC1 and could represent a potential therapeutic strategy for improving hepatic steatosis.

To confirm that the reduced *in vitro* DNL translates *in vivo*, we administered a selective ACC1 inhibitor to C57BL/6J mice. Hepatic M-CoA concentrations negatively correlated with the plasma concentration of compound-1 and fatty acid synthesis, which were measured by the incorporation of acetate into lipids, was significantly suppressed by compound-1 treatment (10 mg/kg; Figure 2 and

JPET Fast Forward. Published on September 17, 2021 as DOI: 10.1124/jpet.121.000786
This article has not been copyedited and formatted. The final version may differ from this version.

Supplementary Table 1). In addition, we confirmed the ACC1 selectivity for compound-1 *in vivo* by comparing its effect on the reduction in M-CoA levels in the liver and muscles. These results support that compound-1 inhibits DNL via ACC1 inhibition *in vivo* and corroborates the *in vitro* results.

We also evaluated the impact of ACC1 inhibition on steatosis and fibrosis through repeated compound-1 dosing in a genetic and diet-induced WD-fed MC4R KO mouse model. This model shows multiple histopathological features common to NASH patients, including hepatic steatosis, inflammation, and fibrosis. Further, the expression of liver lipogenesis-related genes, including *ACC1*, are elevated in this mouse model compared to WT control mice (Itoh et al., 2011; Konuma et al., 2015; Shiba et al., 2018). The reported pathological features in this model were also noted in our WD-fed MC4R KO mice. In contrast to the increased *ACC1* expression, expression of *ACC2* was unchanged in the livers of model mice compared to that in WT mice (Supplementary Figure 1). This is consistent with the findings of a previous study on human NAFLD patients (Kohjima et al., 2007), suggesting that ACC1 might contribute more strongly to NAFLD progression than ACC2.

Following 8 weeks of compound-1 treatment, hepatic TG accumulation was attenuated and plasma AST and ALT levels were significantly reduced, indicating that ACC1 inhibition improved hepatic steatosis resulting in ameliorated hepatocellular damage. Furthermore, compound-1 reduced the mRNA expression of genes related to inflammation and collagen synthesis marker levels, hepatic collagen content, and Sirius red-positive area, suggesting that ACC1 inhibition can also reduce inflammation and fibrosis progression either directly by its inhibition in non-hepatocytes or indirectly by reducing the hepatic lipid

JPET Fast Forward. Published on September 17, 2021 as DOI: 10.1124/jpet.121.000786
This article has not been copyedited and formatted. The final version may differ from this version.

content (Bates et al., 2020). Indeed, we observed a correlation between reduced M-CoA concentration via ACC1 inhibition and reduced hepatic TG and collagen content. Cumulatively, these results suggest that inhibiting hepatic DNL by selective ACC1 inhibition may represent a viable strategy for treating NAFLD/NASH.

Although the Sirius red-positive area was not reduced following treatment with 30 mg/kg of compound-1, this may not be attributed to the diminished antifibrotic efficacy but rather, the remarkable improvement of liver hypertrophy, which increases the total analysis area per analysis unit screen at 30 mg/kg compared to that in the other groups. Indeed, fibrosis gene expression and total hepatic collagen content were dose-dependently decreased following compound-1 treatment. However, further studies are needed to address the discrepancy between the hepatic collagen content and Sirius red-positive area.

BW loss was observed in WD-fed MC4R KO mice treated with 30 mg/kg compound-1 compared to vehicle-treated mice. Although the improvement in hepatic hypertrophy could be partially considered as a cause of the BW loss, we hypothesize that compound-dependent toxicities account for the primary cause at the highest dose. Heterozygous ACC1 mutant mice and liver-specific ACC1-deficient mice did not show BW reduction compared to WT mice (Abu-Elheiga et al., 2005; Harada et al., 2007) indicating that the inhibition of ACC1 in the liver is not responsible for the reduced BW. We further evaluated the specificity of compound-1 for 72 panels, including G-protein-coupled receptor, kinase, non-kinase enzyme, ion channel, transporter, and nuclear hormone receptor up to concentrations of 10 μM, and the compound corresponded to only 5-hydroxytryptamine receptor 2B (HTR2B) (IC_{50} = 3.3 μM; data not shown).

JPET Fast Forward. Published on September 17, 2021 as DOI: 10.1124/jpet.121.000786
This article has not been copyedited and formatted. The final version may differ from this version.

However, this efficacy of HTR2B is not expected to have contributed to the observed *in vivo* toxicity as the estimated unbound fraction-based C_{max} at 30 mg/kg in WD-fed MC4R KO mice was less than 160 nM, which was > 20-fold lower than the *in vitro* IC_{50} against HTR2B.

We were unable to discern the impact of weight loss observed with 30 mg/kg compound-1 on the improvement in NASH caused by ACC1 inhibition. Previously we confirmed that 15% calorie restriction resulted in 11.6% reduction in BW without significantly reducing plasma ALT and AST levels or hepatic collagen content in WD-fed MC4R KO mice compared to animals fed *ad libitum* (data not shown). However, marked BW loss (> 10%) improved fibrosis in NAFLD/NASH patients (Mummadi et al., 2008, Glass et al., 2015). Therefore, further studies are needed to confirm whether BW loss or ACC1 inhibition was responsible for the anti-NASH effect of compound-1 at 30mg/kg.

Many pre-clinical and clinical studies have shown that ACC1/2 dual inhibitors increase plasma TG concentrations, which may be a signaling cascade that upregulates TG re-esterification genes and flux (Kim et al., 2017; Bergman et al., 2020; Mitsuharu et al., 2020; Chen et al., 2019; Goedeke l et al., 2018). Indeed, compound-1 significantly increased the expression of ACC1, *Fasn*, and *Scd1*, which are SREBP1c target genes. However, compound-1 did not significantly elevate plasma TG concentrations compared to WT mice (Table 2). We also confirmed that repeated compound-1 dosing for 8 weeks did not increase plasma TG levels in the AMLN diet-fed DIO-NASH model, a diet-induced pre-clinical NAFLD/NASH mouse model, compared to those in lean and vehicle-treated mice (data not shown). As serum TG concentrations are not increased by ACC1/2 inhibitors at a dose that partially inhibits hepatic DNL

JPET Fast Forward. Published on September 17, 2021 as DOI: 10.1124/jpet.121.000786
This article has not been copyedited and formatted. The final version may differ from this version.

(Bergman et al., 2020), and the cellular specific hepatic M-CoA level is compensated by ACC2 activity under ACC1 inhibition conditions (Mao et al., 2006; Harada et al., 2007), one possible explanation for this difference in plasma TG elevation between ACC1/2 inhibitors and a selective ACC1 inhibitor might be that the latter is unable to fully suppress hepatic M-CoA production due to the flux via ACC2. In our study, the maximum M-CoA-lowering effect by selective ACC1 inhibition was less than that by ACC1/2 inhibition. In addition, hepatic ACC2 expression was dose-dependently induced by compound-1 after repeated dosing in WD-fed MC4R KO mice (Supplementary Figure 1). Although further investigations are required, these data suggest that a selective ACC1 inhibitor could improve hepatic steatosis and fibrosis without causing plasma TG elevation as ACC2 compensates the hepatic M-CoA level under ACC1 inhibition, thereby preventing any secondary feedback including increased circulating TGs.

In conclusion, to our knowledge, this is the first study to show that a selective ACC1 inhibitor has sufficient efficacy in pre-clinical models, thus providing a viable approach for treating NAFLD/NASH. The data demonstrate a robust reduction in hepatic steatosis and fibrosis in our pre-clinical animal models. In addition, selective ACC1 inhibition mitigates the increased TG concentrations observed with ACC1/2 inhibitors in clinical studies. These findings support the ACC1 inhibitor as a potential novel treatment for NAFLD/NASH.

JPET Fast Forward. Published on September 17, 2021 as DOI: 10.1124/jpet.121.000786
This article has not been copyedited and formatted. The final version may differ from this version.

Acknowledgments

The authors are grateful to Nobuyuki Amano, Yuichiro Amano, Ryo Mizojiri, and Noboru Tsuchimori from the Pharmaceutical Research Division, Takeda Pharmaceutical Company Limited, Kanagawa, Japan, and Noriko Uchiyama from Global Drug Safety Research Evaluation, Takeda Pharmaceutical Company Limited, Cambridge, USA for their guidance and valuable comments. The authors would like to acknowledge all Takeda ACC1 project members, especially Kazue Tsuchimori and Sayaka Nakagawa from the Pharmaceutical Research Division, Takeda Pharmaceutical Company Limited, Kanagawa, Japan.

Author contributions

Participated in research design: Tamura, Sugama, Iwasaki, Sasaki, Yasuno, Aoyama, Watanabe, Erion, and Yashiro.

Conducted Experiments: Tamura, Sugama, Iwasaki, Sasaki, Yasuno, Aoyama, and Yashiro.

Performed data analysis: Tamura, Sugama, Iwasaki, Sasaki, Yasuno, Aoyama, and Yashiro.

Wrote or contributed to the writing of the manuscript: Tamura, Sugama, Iwasaki, Sasaki, Yasuno, Aoyama, Watanabe, Erion, and Yashiro.

References

Abu-Elheiga L, Matzuk MM, Abo-Hashema KA, and Wakil SJ (2001) Continuous fatty acid oxidation and reduced fat storage in mice lacking acetyl-CoA carboxylase 2. Science 291: 2613-2616.

Abu-Elheiga L, Oh W, Kordari P, and Wakil SJ (2003) Acetyl-CoA carboxylase 2 mutant mice are protected against obesity and diabetes induced by high-fat/high-carbohydrate diets. Proc Natl Acad Sci U S A 100: 10207-10212.

Abu-Elheiga L, Matzuk MM, Kordari P, Oh W, Shaikenov T, Gu Z, and Wakil SJ (2003) Mutant mice lacking acetyl-CoA carboxylase 1 are embryonically lethal. Proc Natl Acad Sci U S A 102: 12011-12016.

Anstee QM, Targher G, and Day CP (2013) Progression of NAFLD to diabetes mellitus, cardiovascular disease or cirrhosis. Nat Rev Gastroenterol Hepatol 10: 330-344.

Bates J, Vijayakumar A, Ghoshal S, Marchand B, Yi S, Kornyeyev D, Zagorska A, Hollenback D, Walker K, Liu K, Pendem S, Newstrom D, Brockett R, Mikaelian I, Kusam S, Ramirez R, Lopez D, Li L, Fuchs BC, and Brechenridge DG (2020) Acetyl-CoA carboxylase inhibition disrupts metabolic reprogramming during hepatic stellate cell activation. J Hepatol 73: 896-905.

Bergman A, Carvajal-Gonzalez S, Tarabar S, Saxena AR, Esler WP, and Amin NB (2020) Safety, tolerability, pharmacokinetics, and pharmacodynamics of a liver-targeting acetyl-CoA carboxylase inhibitor (PF-05221304): A three-part randomized phase 1 study. Clin Pharmacol Drug Dev 9: 514-526.

Brownsey RW, Zhande R, and Boone AN (1997) Isoforms of acetyl-CoA carboxylase: structures, regulatory properties and metabolic functions. Biochem Soc Trans 25: 1232-1238.

Bertot LC and Adams LA (2016) The natural course of non-alcoholic fatty liver disease. Int J Mol Sci 17: 774.

Chen L, Duan Y, Wei H, Ning H, Bi C, Zhao Y, Qin Y, and Li Y (2019) Acetyl-CoA carboxylase (ACC) as a therapeutic target for metabolic syndrome and recent developments in ACC1/2 inhibitors. Expert Opin Investig Drugs 28: 917-930.

Choi CS, Savage DB, Abu-Elheiga L, Liu Z, Kim S, Kulkarni A, Distefano A, Hwang YJ, Reznick RM, Codella R, and Zhang D (2007) Continuous fat oxidation in acetyl–CoA carboxylase 2 knockout mice increases total energy expenditure, reduces fat mass, and improves insulin sensitivity. Proc Natl Acad Sci U S A 104: 16480-16485.

Cohen JC, Horton JD, and Hobbs HH (2011) Human fatty liver disease: old questions and new insights Science 332: 1519-1523.

Cusi K, Orsak B, Bril F, Lomonaco R, Hecht J, Ortiz-Lopez C, Tio F, Hardies J, Darland C, Musi N, Webb A, and Portillo-Sanchez P (2016) Long-term pioglitazone treatment for patients with nonalcoholic steatohepatitis and prediabetes or type 2 diabetes mellitus. Ann Intern Med 165: 305-315.

Donnelly KL, Smith CI, Schwarzenberg SJ, Jessurun J, Boldt MD, and Parks EJ (2005) Sources of fatty acids stored in liver and secreted via lipoproteins in patients with nonalcoholic fatty liver disease. J Clin Invest 115: 1343-1351.

Esler WP and Bence KK (2019) Metabolic targets in nonalcoholic fatty liver disease. Cell Mol Gastroenterol Hepatol 8: 247-267.

Fabbrini E, Mohammed BS, Magkos F, Korenblat KM, Patterson BW, and Klein S (2008) Alterations in adipose tissue and hepatic lipid kinetics in obese men and women with nonalcoholic fatty liver disease. Gastroenterology 134: 424-431.

Friedman SL, Neuschwander-Tetri BA, Rinella M, and Sanyal AJ (2018) Mechanisms of NAFLD

development and therapeutic strategies. Nat Med 24: 908-922

Glass LM, Dickson RC, Anderson JC, Suriawinata AA, Putra J, Berk BS, and Toor A (2015) Total body weight loss of ≥ 10 % is associated with improved hepatic fibrosis in patients with nonalcoholic steatohepatitis. Dig Dis Sci 60: 1024-1030.

Glien M, Haschke G, Schroeter K, Pfenninger A, Zoller G, Keil S, Müller M, Herling AW, and Schmoll D (2011) Stimulation of fat oxidation, but no sustained reduction of hepatic lipids by prolonged pharmacological inhibition of acetyl CoA carboxylase. Horm Metab Res 43: 601-606.

Goedeke L, Bates J, Vatner DF, Perry RJ, Wang T, Ramirez R, Li L, Ellis MW, Zhang D, Wong KE, Beysen C, Cline GW, Ray AS, and Shulman GI (2018) Acetyl-CoA carboxylase inhibition reverses NAFLD and hepatic insulin resistance but promotes hypertriglyceridemia in rodents. Hepatology 68: 2197-2211.

Harada N, Oda Z, Hara Y, Fujinami K, Okawa M, Ohbuchi K, Yonemoto M, Ikeda Y, Ohwaki K, Aragane K, Tamai Y, and Kusunoki J (2007) Hepatic de novo lipogenesis is present in liver-specific ACC1-deficient mice. Mol Cell Biol 27: 1881-1888.

Harriman G, Greenwood J, Bhat S, Huang X, Wang R, Paul D, Tong L, Saha AK, Westlin WF, Kapeller R, and Harwood HJ Jr (2006) Acetyl-CoA carboxylase inhibition by ND-630 reduces hepatic steatosis, improves insulin sensitivity, and modulates dyslipidemia in rats. Proc Natl Acad Sci U S A 113: E1796-1805.

Harwood HJ Jr, Petras SF, Shelly LD, Zaccaro LM, Perry DA, Makowski MR, Hargrove DM, and Martin KA (2003) Isozyme-nonselective N-substituted bipiperidylcarboxamide acetyl-CoA carboxylase inhibitors reduce tissue malonyl-CoA concentrations, inhibit fatty acid synthesis, and increase fatty acid oxidation in cultured cells and in experimental animals. J Biol Chem 278: 37099-37111.

Itoh M, Suganami T, Nakagawa N, Tanaka M, Yamamoto Y, Kamei Y, Terai S, Sakaida I, and Ogawa Y (2011) Melanocortin 4 receptor-deficient mice as a novel mouse model of nonalcoholic steatohepatitis. Am J Pathol 179: 2454-2463.

Kamata M, Yamashita T, Kina A, Tawada M, Endo S, Mizukami A, Sasaki M, Tani A, Nakano Y, Watanabe Y, Furuyama N, Funami M, Amano N, and Fukatsu K (2012) Symmetrical approach of spiro-pyrazolidinediones as acetyl-CoA carboxylase inhibitors. Bioorg Med Chem Lett 22: 4769-4772.

Kim CW, Addy C, Kusunoki J, Anderson NN, Deja S, Fu X, Burgess SC, Li C, Ruddy M, Chakravarthy M,

Previs S, Milstein S, Fitzgerald K, Kelley DE, and Horton JD (2017) Acetyl CoA carboxylase inhibition reduces hepatic steatosis but elevates plasma triglycerides in mice and humans: a bedside to bench investigation. Cell Metab 26: 394-406.e6

Kohjima M, Enjoji M, Higuchi N, Kato M, Kotoh K, Yoshimoto T, Fujino T, Yada M, Yada R, Harada N, Takayanagi R, and Nakamuta M (2007) Re-evaluation of fatty acid metabolism-related gene expression in nonalcoholic fatty liver disease. Int J Mol Med 20: 351-358.

Konuma K, Itoh M, Suganami T, Kanai S, Nakagawa N, Sakai T, Kawano H, Hara M, Kojima S, Izumi Y, and Ogawa Y (2015) Eicosapentaenoic acid ameliorates non-alcoholic steatohepatitis in a novel mouse model using melanocortin 4 receptor-deficient mice. PLoS One 10: e0121528.

Lambert JE, Ramos-Roman MA, Browning JD, and Parks EJ (2014) Increased de novo lipogenesis is a distinct characteristic of individuals with nonalcoholic fatty liver disease. Gastroenterology 146: 726-35.

Mao J, DeMayo FJ, Li H, Abu-Elheiga L, Gu Z, Shaikenov TE, Kordari P, Chirala SS, Heird WC, and Wakil SJ (2006) Liver-specific deletion of acetyl-CoA carboxylase 1 reduces hepatic triglyceride accumulation without affecting glucose homeostasis. Proc Natl Acad Sci U S A 103: 8552-8557.

Matsumoto M, Yashiro H, Ogino H, Aoyama K, Nambu T, Nakamura S, Nishida M, Wang X, Erion DM, and Kaneko M (2020) Acetyl-CoA carboxylase 1 and 2 inhibition ameliorates steatosis and hepatic fibrosis in a MC4R knockout murine model of nonalcoholic steatohepatitis. PLoS One 15: e0228212.

Mizojiri R, Asano M, Tomita D, Banno H, Nii N, Sasaki M, Sumi H, Satoh Y, Yamamoto Y, Moriya T, Satomi Y, and Maezaki H (2018) Discovery of novel selective acetyl-CoA carboxylase (ACC) 1 inhibitors. J Med Chem 61: 1098-1117.

Mummadi RR, Kasturi KS, Chennareddygari S, and Sood GK (2008) Effect of bariatric surgery on nonalcoholic fatty liver disease: systematic review and meta-analysis. Clin Gastroenterol Hepatol 6: 1396-1402.

Savage DB, Choi CS, Samuel VT, Liu Z, Zhang D, Wang A, Zhang XM, Cline GW, Yu XX, Geisler JG, Bhanot S, Monia BP, and Shulman GI (2006) Reversal of diet-induced hepatic steatosis and hepatic insulin resistance by antisense oligonucleotide inhibitors of acetyl-CoA carboxylases 1 and 2. J Clin Invest 116: 817-824.

Sanyal AJ, Chalasani N, Kowdley KV, McCullough A, Diehl AM, Bass NM, Neuschwander-Tetri BA, Lavine JE, Tonascia J, Unalp A, Van Natta M, Clark J, Brunt EM, Kleiner DE, Hoofnagle JH, and Robuck

PR; NASH CRN (2010) Pioglitazone, vitamin E, or placebo for nonalcoholic steatohepatitis. N Engl J Med 362: 1675-1685.

Shiba K, Tsuchiya K, Komiya C, Miyachi Y, Mori K, Shimazu N, Yamaguchi S, Ogasawara N, Katoh M, Itoh M, Suganami T, and Ogawa Y (2018) Canagliflozin, an SGLT2 inhibitor, attenuates the development of hepatocellular carcinoma in a mouse model of human NASH. Sci Rep 8: 2362.

Siddiqui MS, Harrison SA, Abdelmalek MF, Anstee QM, Bedossa P, Castera L, Dimick - Santos L, Friedman SL, Greene K, Kleiner DE, Megnien S, Neuschwander - Tetri BA, Ratziu V, Schabel E, Miller V, and Sanyal AJ on behalf of the Liver Forum Case Definitions Working Group (2018) Case definitions for inclusion and analysis of endpoints in clinical trials for nonalcoholic steatohepatitis through the lens of regulatory science. Hepatology 67: 2001-2012.

Vernon G, Baranova A, and Younossi ZM (2011) Systematic review: the epidemiology and natural history of non-alcoholic fatty liver disease and non-alcoholic steatohepatitis in adults. Aliment Pharmacol Ther 34: 274-285.

Williams CD, Stengel J, Asike MI, Torres DM, Shaw J, Contreras M, Landt CL, and Harrison SA (2011) Prevalence of nonalcoholic fatty liver disease and nonalcoholic steatohepatitis among a largely

middle-aged population utilizing ultrasound and liver biopsy: a prospective study. Gastroenterology 140: 124-131.

Younossi Z, Tacke F, Arrese M, Sharma BC, Mostafa I, Bugianesi E, Wai-Sun Wong V, Yilmaz Y, George J, Fan J, and Vos MB (2019) Global perspectives on nonalcoholic fatty liver disease and nonalcoholic steatohepatitis. Hepatology 69: 2672-2682.

Zechini B, Pasquazzi C, and Aceti A (2004) Correlation of serum aminotransferases with HCV RNA levels and histological findings in patients with chronic hepatitis C: the role of serum aspartate transaminase in the evaluation of disease progression. Eur J Gastroenterol Hepatol 16: 891-896.

JPET Fast Forward. Published on September 17, 2021 as DOI: 10.1124/jpet.121.000786
This article has not been copyedited and formatted. The final version may differ from this version.

Footnotes

This work was supported by Takeda Pharmaceuticals. Among the authors, YOT, SI, MS, HY, and HY are employees of Takeda Pharmaceuticals Inc. and stockholders of Takeda. JS, KA, MW, and DME were employees of Takeda Pharmaceuticals Inc. and stockholders of Takeda at the time of their contribution to the study reported.

Reprint requests should be addressed to Hiroaki Yashiro at the Gastroenterology Drug Discovery Unit, Takeda Pharmaceuticals International Co. 350 Massachusetts Avenue, Cambridge, MA 02139, USA. E-mail: hiroaki.yashiro@takeda.com

JPET Fast Forward. Published on September 17, 2021 as DOI: 10.1124/jpet.121.000786
This article has not been copyedited and formatted. The final version may differ from this version.

Figure Legends

Figure 1. Effect of compound-1 on M-CoA content and fatty acid synthesis in HepG2 cells (A) Effect of compound-1 on M-CoA content in HepG2 cells. (B) Effect of compound-1 on [^{14}C] acetate incorporation into fatty acids in HepG2 cells. Data are presented as the mean ± SD (n = 3).

Figure 2. Effects of single oral dose of compound-1 in C57BL/6J mice. (A) Effect of compound-1 and compound-2 on hepatic malonyl-CoA in normal diet-fed C57BL/6J mice 2 h after a single oral dose. Data are presented as the mean ± SD (n = 5). $^{\$\$\$}$ $p < 0.001$ vs. vehicle by Aspin–Welch test; ** $p < 0.01$, *** $p < 0.001$ vs. vehicle by Dunnett's test. (B) Effect of compound-1 (10 mg/kg) on [^{14}C] acetate incorporation into fatty acids in WD-fed C57BL/6J mice 2 and 5 h after dosing. Data are presented as the mean ± SD (n = 3). $^{\#\#\#}$ $p < 0.001$ vs. vehicle by Student's *t*-test; $^{\$}$ $p < 0.05$ vs. vehicle by Aspin–Welch test.

Figure 3. Effect of chronic compound-1 on liver weight, triglyceride (TG) content, body weight (BW), and food intake (FI) in WD-fed MC4R KO mice. (A) Liver weight, (B) hepatic TG (mg/tissue), (C) BW change at day 56, and (D) cumulative FI at 56 days. Data are presented as the mean ± SD (n = 5–8). $^{\#\#}$ $p < 0.01$ vs. WT by Student's *t*-test; $^{\$\$\$}$ $p < 0.001$ vs. WT by Aspin–Welch test; *** $p < 0.001$ vs. vehicle by Dunnett's test; †† $p < 0.01$ vs. vehicle by Steel's test.

Figure 4. Effect of chronic compound-1 on hepatic mRNA expression in WD-fed MC4R KO mice. Gene expression of (A) *MCP-1*, (B) *F4/80*, (C) *Col1α1*, (D) *Col1α2*, (E) *αSMA*, and (F) *TGF-β1*. Data are presented as the mean ± SD (n = 5–8). $^{\#}$ $p < 0.05$, $^{\#\#\#}$ $p < 0.001$ vs. WT by Student's *t*-test; $^{\$\$\$}$ $p < 0.001$ vs. WT by Aspin–Welch test; * $p < 0.05$ vs. vehicle by Dunnett's test; † $p < 0.05$, †† $p < 0.01$ vs. vehicle by

JPET Fast Forward. Published on September 17, 2021 as DOI: 10.1124/jpet.121.000786
This article has not been copyedited and formatted. The final version may differ from this version.

Steel's test.

Figure 5. Effect of chronic compound-1 on total hepatic M-CoA content in WD-fed MC4R KO mice.

Data are presented as the mean ± SD (n = 5–8). *** $p < 0.001$ vs. vehicle by Dunnett's test.

Figure 6. Effect of chronic compound-1 on liver fibrosis in WD-fed MC4R KO mice. (A) Total hepatic collagen content, (B) Sirius red-positive area, (C) Representative images of liver sections stained with Sirius red (magnification 10×, scale bar = 100 μm), (D) Correlation between hepatic M-CoA and hepatic TG, and (E) Correlation between hepatic M-CoA and hepatic collagen. Data are presented as the mean ± SD (n = 5–8). $^{###}$ $p < 0.001$ vs. WT by Student's *t*-test; $^{\$\$\$}$ $p < 0.001$ vs. WT by Aspin–Welch test; * $p < 0.05$, ** $p < 0.01$, *** $p < 0.001$ vs. vehicle by Dunnett's test.

JPET Fast Forward. Published on September 17, 2021 as DOI: 10.1124/jpet.121.000786
This article has not been copyedited and formatted. The final version may differ from this version.

Tables

Table 1. Inhibitory activity of compound-1 and compound-2 on recombinant mouse ACC1 and ACC2 proteins

	mACC1 IC_{50} (nM)	**mACC2 IC_{50} (nM)**
Compound-1	1.9	> 10,000
Compound-2	6.0	6.4

JPET Fast Forward. Published on September 17, 2021 as DOI: 10.1124/jpet.121.000786
This article has not been copyedited and formatted. The final version may differ from this version.

Table 2. Effect of chronic compound-1 on plasma parameters in WD-fed MC4R KO mice

Mice		WT	WD-fed MC4R KO			
Treatment		Vehicle (n=5)	Vehicle (n=8)	Compound-1		
				3 mg/kg (n=8)	10 mg/kg (n=8)	30 mg/kg (n=8)
AST (IU/L)	Pre	41.8 ± 7.0	636.9 ± 96.4 $^{\$\$\$}$	601.7 ± 108.6	613.2 ± 101.7	620.7 ± 92.3
	Post	64.3 ± 12.8	649.6 ± 86.7	526.4 ± 84.6 $^{\text{⁋}}$	268.9 ± 61.7 $^{\text{⁋⁋}}$	105.3 ± 8.0 $^{\text{⁋⁋}}$
ALT (IU/L)	Pre	22.1 ± 4.6	857.6 ± 103.9 $^{\$\$\$}$	849.5 ± 133.2	860.2 ± 118.8	858.9 ± 113.1
	Post	20.4 ± 14.1	840.7 ± 124.4	612.2 ± 94.2 $^{\text{⁋}}$	283.9 ± 74.0 $^{\text{⁋⁋}}$	54.6 ± 9.1 $^{\text{⁋⁋}}$
TG (mg/dL)	Pre	132.0 ± 16.0	85.1 ± 15.9 $^{\#\#\#}$	88.2 ± 22.7	75.5 ± 15.1	81.7 ± 25.8
	Post	117.5 ± 39.6	75.2 ± 9.3	132.0 ± 36.2 $^{\text{⁋⁋}}$	146.0 ± 31.9 $^{\text{⁋⁋}}$	159.3 ± 73.8 $^{\text{⁋⁋}}$
T-Cho (mg/dL)	Pre	95.5 ± 6.2	405.5 ± 22.4 $^{\$\$\$}$	393.1 ± 38.3	387.2 ± 26.6	403.0 ± 31.3
	Post	97.0 ± 5.0	429.2 ± 18.6	390.4 ± 37.7 *	305.3 ± 37.2 ***	164.8 ± 25.4 ***

[a]Plasma parameters were measured before (Pre) and after (Post) 8 weeks of treatment.

[b]Data are presented as the mean ± SD (n = 5–8).

$^{\#\#\#}$ $p < 0.001$ vs. WT by Student's *t*-test, $^{\$\$\$}$ $p < 0.001$ vs. WT by Aspin–Welch test.

* $p < 0.05$, *** $p < 0.001$ vs. vehicle by Dunnett's test.

$^{\text{⁋}}$ $p < 0.05$, $^{\text{⁋⁋}}$ $p < 0.01$ vs. vehicle by Steel's test.

JPET Fast Forward. Published on September 17, 2021 as DOI: 10.1124/jpet.121.000786
This article has not been copyedited and formatted. The final version may differ from this version.

Figure 1

JPET Fast Forward. Published on September 17, 2021 as DOI: 10.1124/jpet.121.000786
This article has not been copyedited and formatted. The final version may differ from this version.

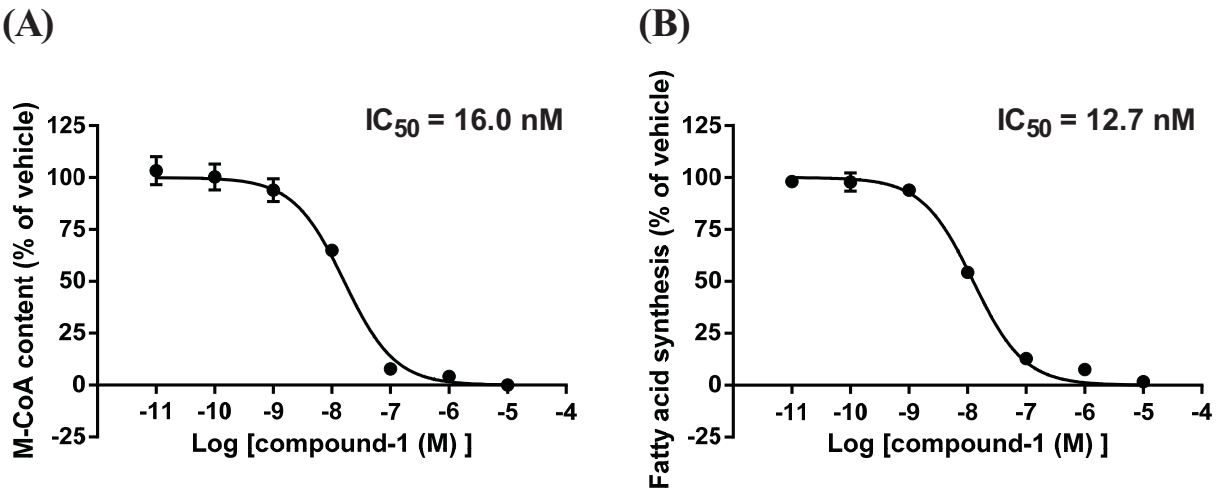

JPET Fast Forward. Published on September 17, 2021 as DOI: 10.1124/jpet.121.000786
This article has not been copyedited and formatted. The final version may differ from this version.

Figure 2

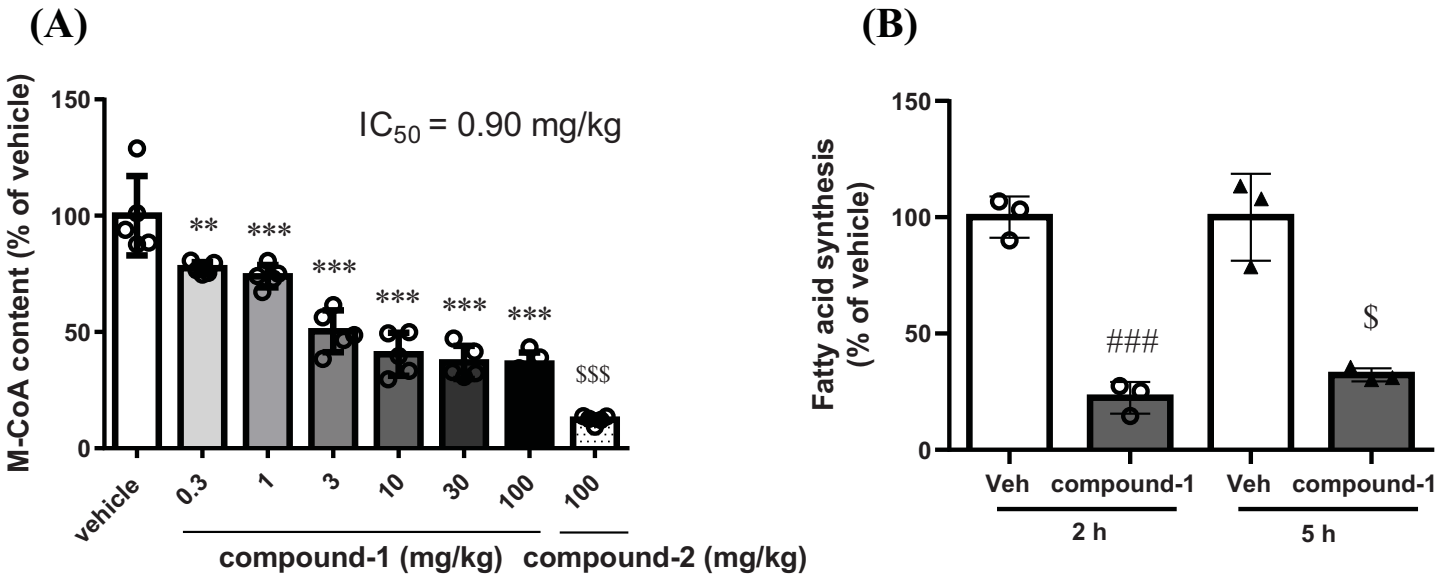

JPET Fast Forward. Published on September 17, 2021 as DOI: 10.1124/jpet.121.000786
This article has not been copyedited and formatted. The final version may differ from this version.

Figure 3

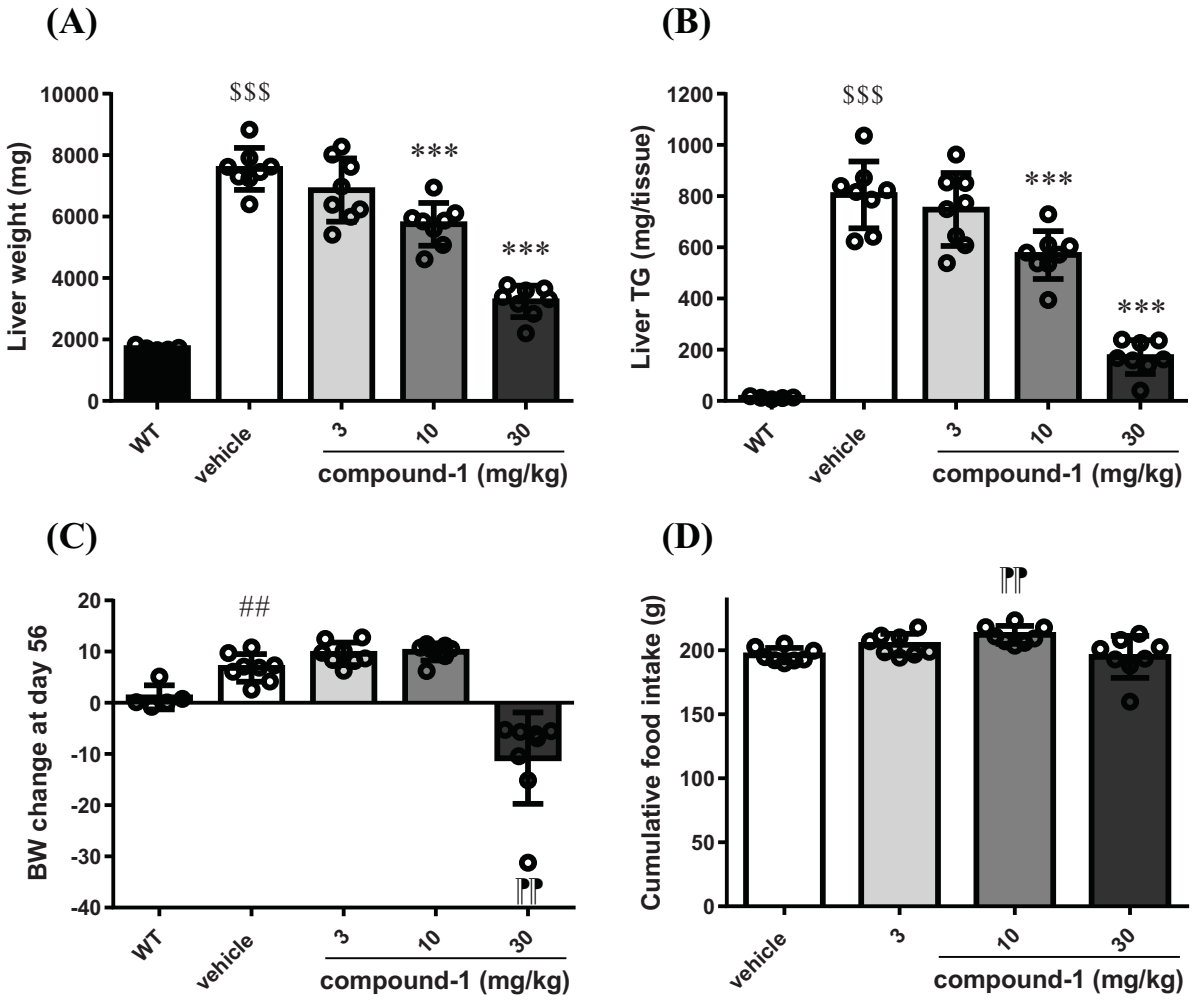

JPET Fast Forward. Published on September 17, 2021 as DOI: 10.1124/jpet.121.000786
This article has not been copyedited and formatted. The final version may differ from this version.

Figure 4

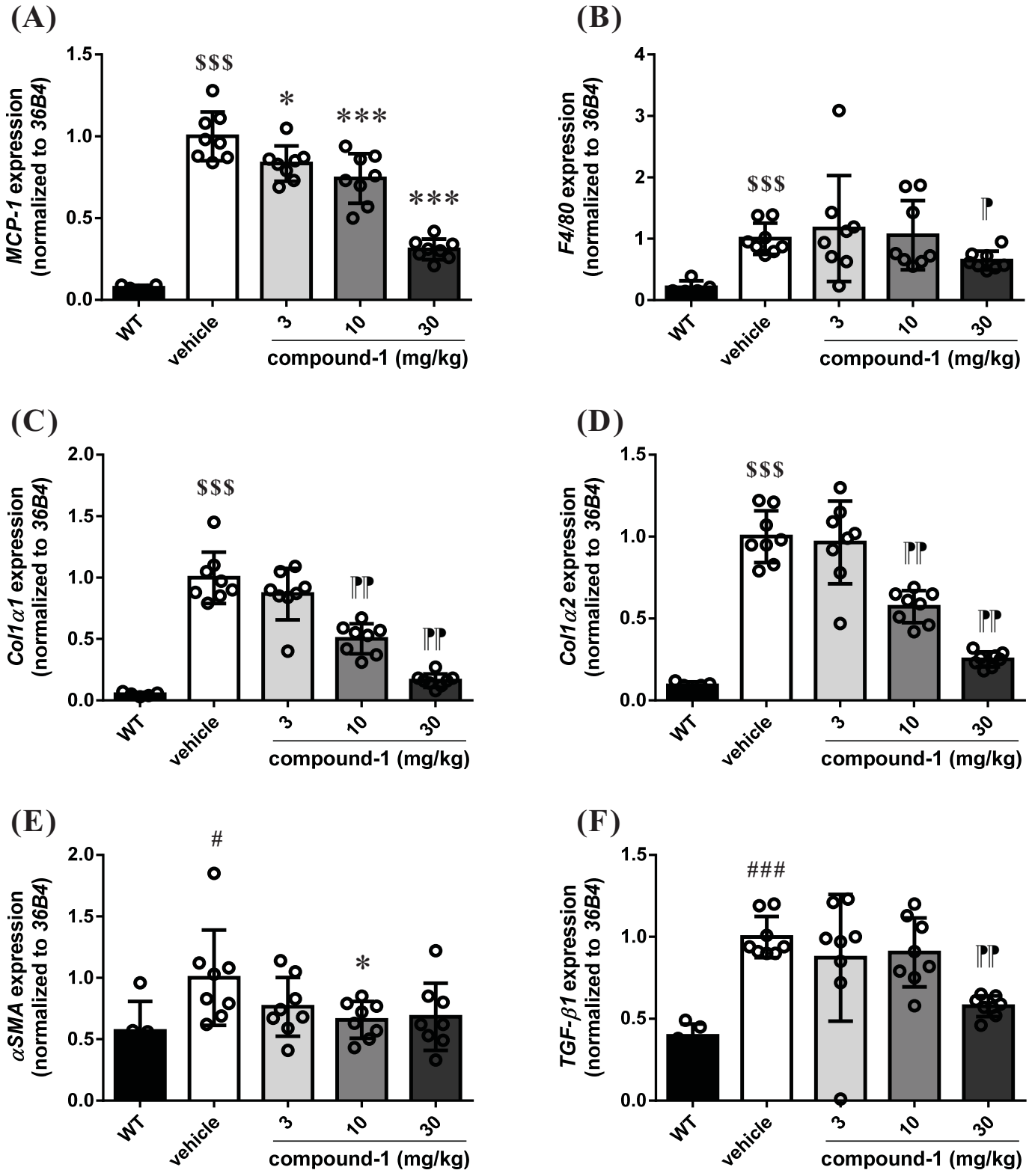

Figure 5

JPET Fast Forward. Published on September 17, 2021 as DOI: 10.1124/jpet.121.000786
This article has not been copyedited and formatted. The final version may differ from this version.

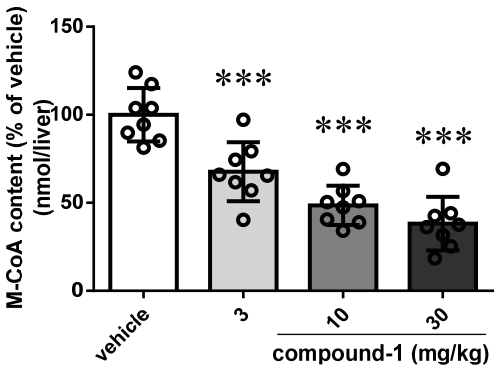

JPET Fast Forward. Published on September 17, 2021 as DOI: 10.1124/jpet.121.000786
This article has not been copyedited and formatted. The final version may differ from this version.

Figure 6

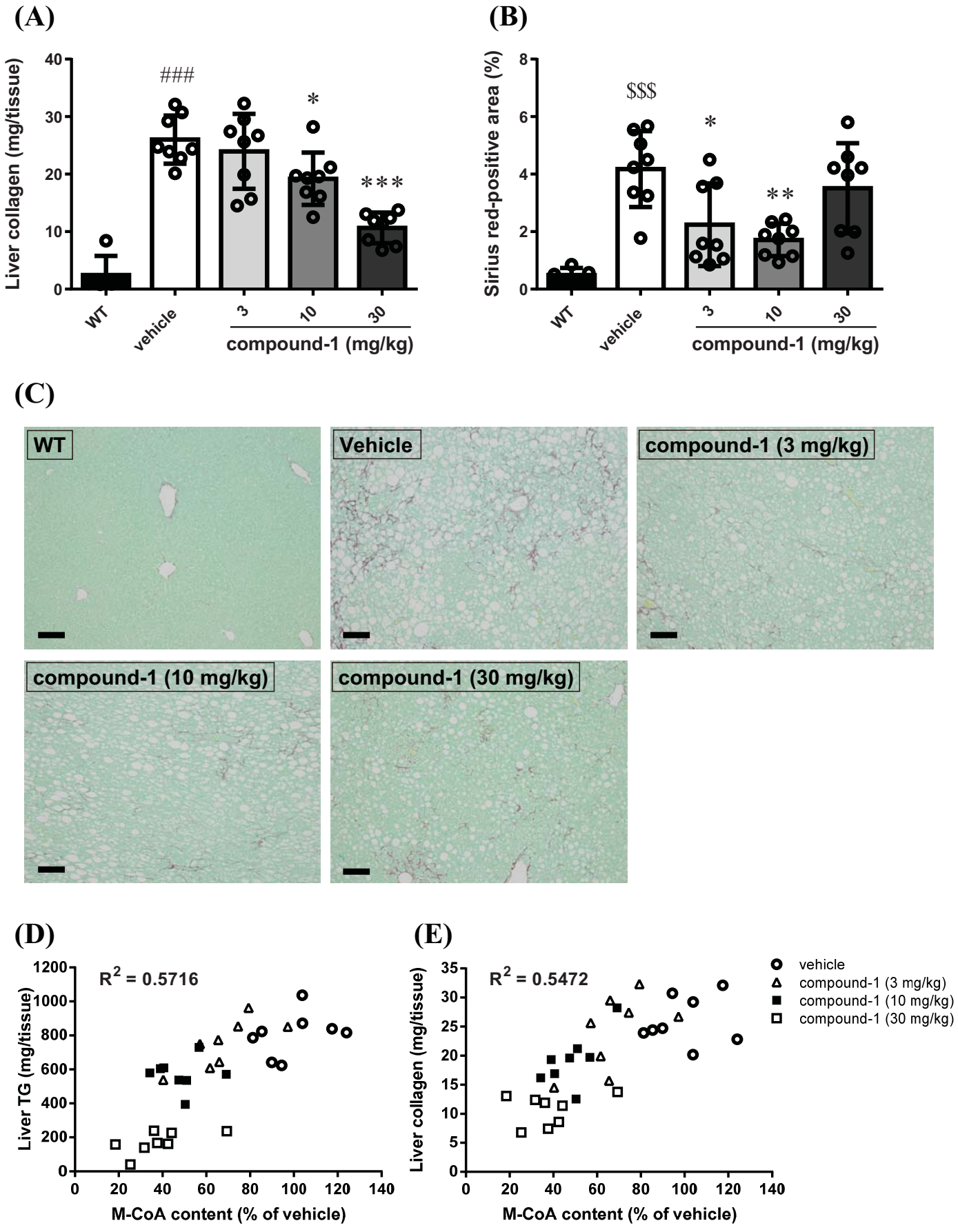

SUPPLEMENTARY INFORMATION

Manuscript No.: JPET-AR-2021-000786

Selective acetyl CoA carboxylase 1 inhibitor improves hepatic steatosis and fibrosis in a pre-clinical NASH model

Yumiko Okano Tamura, Jun Sugama, Shinji Iwasaki, Masako Sasaki, Hironobu Yasuno, Kazunobu Aoyama, Masanori Watanabe, Derek M. Erion, Hiroaki Yashiro

Supplementary Materials and Methods

Measurement of pharmacokinetics in mice

Plasma concentrations of compound-1 were measured using the LC/MS/MS method. Plasma was precipitated using acetonitrile containing the internal standard, diclofenac. The precipitated sample was centrifuged for 5 min at approximately 3000 × *g*. The supernatants were diluted with the mobile phase and injected into the LC/MS/MS system. This system comprised a 20AD-VP system (Shimadzu, Kyoto, Japan) and a triple quadrupole mass spectrometry detection API-5000 (AB Sciex, Framingham, MA, USA), equipped with a turbo ion spray ionization source in the positive ionization mode. Chromatographic separation was achieved using a reversed phase (C18) column [Shim-pack XR-ODS (2.2 μm, 2.0 × 30 mm); Shimadzu, Kyoto, Japan] at 50 °C. The mobile phase consisted of 0.2% (v/v) formic acid in 0.01 M ammonium formate (pH 3.0; solvent A) and 0.2% (v/v) formic acid in acetonitrile (solvent B), which was delivered at a flow rate of 0.7 mL/min. The analyte was eluted using a linear gradient of 95% solvent A/5% solvent B to 5% solvent A/95% solvent B. Detection was performed using multiple reaction monitoring in the positive ionization mode (SRM m/z = 424.2 → 101.1 for T-3773082 and m/z = 296.1 → 214.2 for diclofenac). Analyst software™ (version 1.6.2; AB Sciex) was used for data acquisition and processing. The concentration of compounds in each sample was back calculated using a calibration curve generated from a set of calibration standards.

Supplementary data

Supplementary Table S1. Plasma compound-1 concentration in normal-fed C57BL/6J mice 2 h after oral administration

Dose (mg/kg)	Plasma concentration (μg/mL)	
	Mean	SD
0.3	0.686	0.119
1	2.243	0.367
3	6.045	0.981
10	18.762	2.957
30	51.018	3.438
100	115.174	3.555

Data are presented as the mean ± SD (n = 5)

Supplementary Table S2. Plasma concentration and pharmacokinetic parameters of compound-1 in the plasma of WD-fed MC4R KO mice after 8 weeks of repeated oral administration

(A)

Time (h)	Plasma concentration (μg/mL)					
	3 mg/kg		10 mg/kg		30 mg/kg	
	Mean	SD	Mean	SD	Mean	SD
0	2.138	0.023	5.891	0.832	16.519	2.840
0.5	6.699	1.349	21.532	2.040	41.969	7.436
1	8.427	1.336	23.485	0.497	44.202	16.166
2	8.239	0.384	25.918	7.103	66.524	9.868
6	5.679	0.196	19.836	0.840	60.414	2.923

(B)

Dose	3 mg/kg	10 mg/kg	30 mg/kg
C_{max} (μg/mL)	8.427	25.918	66.524
T_{max} (h)	1.00	2.00	2.00
$AUC_{0–6\ h}$ (μg·h/mL)	42.160	134.320	345.404
MRT (h)	2.78	2.91	3.19

Data are presented as the mean ± SD (n = 3).

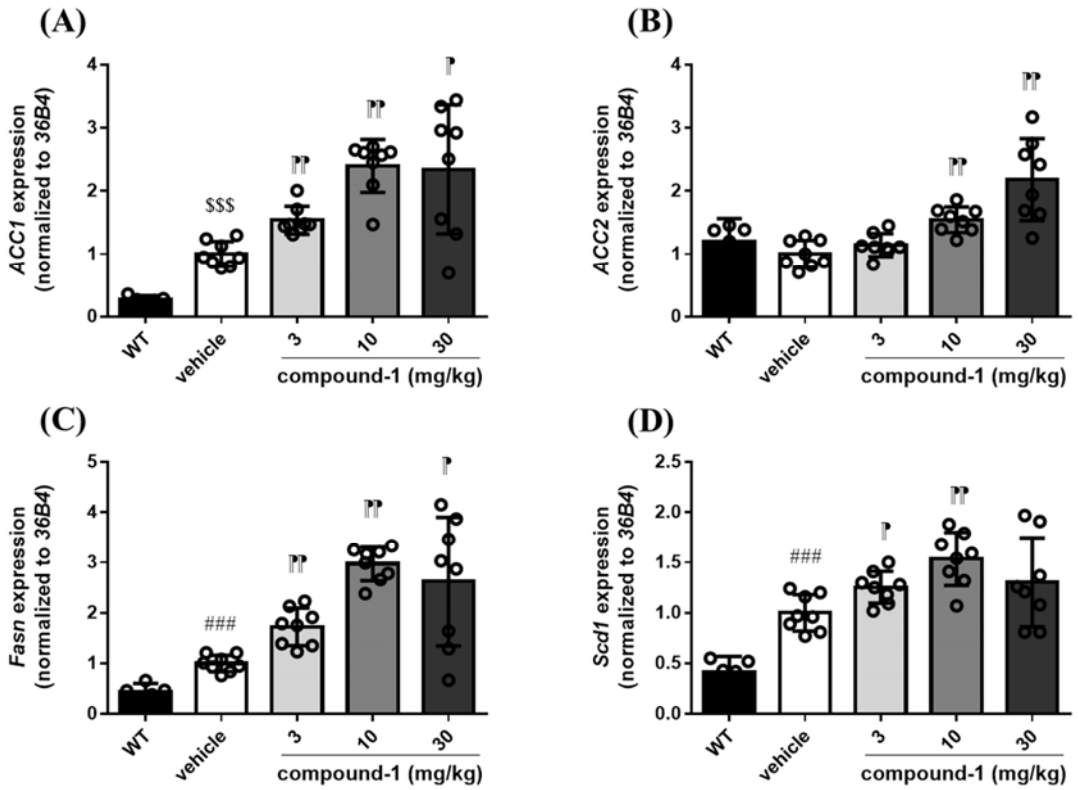

Supplementary Figure S1. Effect of chronic compound-1 on hepatic mRNA expression in WD-fed MC4R KO mice. Gene expression of (A) *ACC1*, (B) *ACC2*, (C) *Fasn*, and (D) *Scd1*. Data are presented as the mean ± SD (n = 5–8). $^{###}$ $p < 0.001$ vs. WT by Student's *t*-test; $^{\$\$\$}$ $p < 0.001$ vs. WT by Aspin–Welch test; $^{⁋}$ $p < 0.05$, $^{⁋⁋}$ $p < 0.01$ vs. vehicle by Steel's test.